Journal of Hazardous Materials 387 (2020) 121985

Contents lists available at ScienceDirect

Journal of Hazardous Materials

journal homepage: www.elsevier.com/locate/jhazmat

Dissipation of antibiotics by microalgae: Kinetics, identification of transformation products and pathways

Claude Kiki[a,b,1], Azhar Rashid[a,c,1], Yuwen Wang[a,b], Yan Li[a,b], Qiaoting Zeng[a], Chang-Ping Yu[a,d], Qian Sun[a,*]

[a] CAS Key Laboratory of Urban Pollutant Conversion, Institute of Urban Environment, Chinese Academy of Sciences, China
[b] University of Chinese Academy of Sciences, China
[c] Nuclear Institute for Food and Agriculture, Tarnab, Peshawar 25000, Pakistan
[d] Graduate Institute of Environmental Engineering, National Taiwan University, Taiwan

GRAPHICAL ABSTRACT

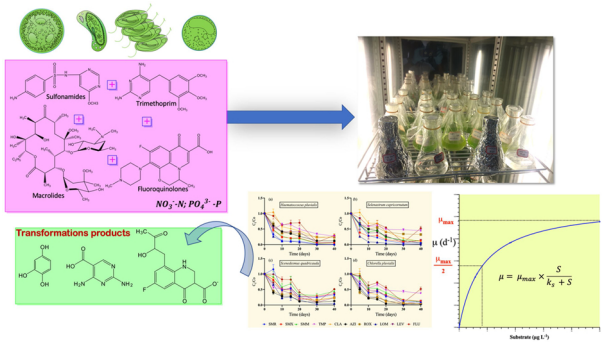

ARTICLE INFO

Editor: R Sara

Keywords:
Microalgae batch culture
Antibiotic dissipation
Monod kinetics
Transformation products

ABSTRACT

Dissipation potential of four algae viz. *Haematococcus pluvialis, Selenastrum capricornutum, Scenedesmus quadricauda* and *Chlorella vulgaris* was investigated against ten antibiotics (sulfamerazine, sulfamethoxazole, sulfamonomethoxine, trimethoprim, clarithromycin, azithromycin, roxithromycin, lomefloxacin, levofloxacin and flumequine) in a series of synthetic wastewater batch culture experiments, maintained at 20, 50 and 100 μg L^{-1} initial concentration levels and incubated over a period of 40 days. Generally, the antibiotic removal was achieved with overall dissipation percentage (%) varying among the algal species and different antibiotics. Biodegradation was the major antibiotic removal mechanism from the dissolved fraction, with minor contributions of bioadsorption, bioaccumulation, and abiotic factors. The antibiotics dissipation followed the pseudo-first-order-kinetics with the fastest antibiotic degradation rate achieved by *H. pluvialis*. The Monod kinetics was successfully applied to explain the relationship between the algal growth and the removal of antibiotics and nutrients in the batch cultures. *S. capricornutum* and *C. vulgaris* showed more affinity for the macrolides and fluoroquinolones than sulfonamides, while, *H. pluvialis* and *S. quadricauda* showed relatively higher preference for sulfonamides than the other antibiotic groups. A total of 10 transformation products were identified and the transformation pathway was proposed, accordingly. Most of the transformation products had lower toxicity compared with their parent antibiotics.

* Corresponding author.
E-mail address: qsun@iue.ac.cn (Q. Sun).
[1] Claude Kiki and Azhar Rashid contributed equally to this work.

https://doi.org/10.1016/j.jhazmat.2019.121985
Received 26 September 2019; Received in revised form 4 December 2019; Accepted 26 December 2019
Available online 28 December 2019

1. Introduction

World-wide demand of antibiotics is increasing indefinitely with increase in population and expansion in livestock sector. The partial metabolism (17–90 %) of antibiotics in humans and animals results in the release of antibiotics through urine and feces (Van Epps and Blaney, 2016; Albero et al., 2018) that ultimately contaminate the aquatic and terrestrial environments. Conventional wastewater treatment, which consists of physical, chemical, and biological processes, has shown a limited amount of removal capacities for many antibiotic compounds (Wang et al., 2018; Ashfaq et al., 2017; Sun et al., 2016). Hence, considering the high mass loads of antibiotic residues in the effluents and sludge (Wang et al., 2018; Ashfaq et al., 2017; Sun et al., 2016), great concerns have been raised due to their persistence and potential environmental risk under the current wastewater treatment technologies.

Due to the inherent N and P rich content of wastewater that can essentially facilitate the growth of microalgae, microalgae-based techniques are being revived in the wastewater treatment for the removal of nutrients and organic contaminants (Nagarajan et al., 2019; Wang et al., 2016). The studies on the removal of sulfonamides by *Scenedesmus obliquus* (Xiong et al., 2019a), removal of cefradine and amoxicillin by *Microcystis aeruginosa* and *Chlorella pyrenoidosa* (Du et al., 2018), removal of cephalosporin antibiotic 7-amino cephalosporanic acid (7-ACA) by *Chlorella sp.* from wastewater (Guo et al., 2016), have provided evidence that microalgae-based technique might be a potential alternate strategy as an additional treatment to improve the wastewater quality. Besides, due to the less sensitivity to thiamphenicol, erythromycin, ampicillin, sulfadimethoxine and norfloxacin, *Chlorella vulgaris* was used for the antibiotic wastewater bioremediation (Eguchi et al., 2004), while, *S. quadricauda* had been used to remove tetracycline, owing to its high bioadsorption capacity (Daneshvar et al., 2018). Remarkably, most assessments of antibiotic biodegradation are piloted using single chemical or few chemicals at high concentrations, while, these chemicals are existent in wastewater effluents in mixtures at relatively low concentration (Hammershøj et al., 2019; Gojkovic et al., 2019). The heterogenous mixtures of organic and inorganic contaminants may show antagonisitc, synergistic, or independent reaction with each other during the removal process of one or more components (Okpokwasili and Nweke, 2005). Therefore, the assessments of the removal efficiencies of a broad range of antibiotics by the microalgae should be further conducted.

In the microalgae treatment process, antibiotics can be removed via different mechanisms. The intracellular and extracellular biodegradation are the most effective ways of organic contaminant removal by microalgae via mainly the enzyme reaction (Xiong et al., 2018). Enzymatic degradation occurs in a biphasic process, where, Cytochrome P450 increases the hydrophilicity of organic compounds (Thies et al., 1996) and makes them more prone for degradation by mono- and/or dioxygenase enzymes in the first phase (Foflonker et al., 2016; Khona et al., 2016). In the second phase, the catalytic reaction by the glutathione-S-transferase enzyme dissipates the organic compounds (Foflonker et al., 2016). The bioadsorption of antibiotics by microalgae cells has also been reported (Daneshvar et al., 2018; Angulo et al., 2018), while, the compounds with cationic groups tend to be adsorbed on the microalgal surface through the electrostatic interaction (Xiong et al., 2018). The bioaccumulation, which is an active process driven by the energy to uptake substrates (Sun et al., 2017; Davis et al., 2015), was also one of the essential ways in the antibiotic removal, including the trimethoprim, sulfamethoxazole and levofloxacin (Bai and Acharya, 2017; Xiong et al., 2017a). In addition, the abiotic reactions including hydrolysis and photolysis also contributed in the antibiotic removal (Guo et al., 2016; Li et al., 2018). Therefore, understanding the removal mechanism of algae under mixed antibiotic environment is of great importance.

The chemometric approaches by employing different kinetic models are useful techniques to explain the contaminant dissipation in batch cultures. Monod kinetics model (Jacques, 1949) can further describe the zero- and first-order biodegradation rates of the analytes and express the dependency of biodegradation rates on the biomass concentration (Okpokwasili and Nweke, 2005). Monod kinetics has been successsfully used to describe the relationship of microalgae in the removal of nutrients (Pala and Bölükbaş, 2005; Xin et al., 2010) and other contaminants (Pala and Bölükbaş, 2005; Dutta et al., 2014). Similar approach was used in the present study to understand the relationship of microalgae in the removal of nutrients and antibiotics.

Although, the monitoring of the antibiotics and the analysis of the degradation kinetics provide useful information on the microalgae performance for antibiotic removal. Yet, the identification of transformation products (TPs) is also important, as the TPs may exist long after the parent antibiotics (Aga et al., 2016). In addition, the TPs of the antibiotics by microalgae-based treatment might show higher toxicity compared to the antibiotic compound (Xiong et al., 2019b; Shi et al., 2018), that can pose potential rise in the environmental risks. Nevertheless, the TPs are often unidentified (Aga et al., 2016). There is knowledge gap on the antibiotic TPs by microalgae treatment. So far, the application of liquid chromatography coupled with high resolution mass spectrometry technique has provided an efficient way to analyze the antibiotic TPs (Jaén-gil et al., 2018). With the help of computer modeling, mass spectral databases, and other data processing tools, the identification of TPs from the complex matrices is becoming more assessable, recently (Aga et al., 2016).

Freshwater microalgae viz. *Haematococcus pluvialis, Selenastrum capricornutum, Scenedesmus quadricauda* and *Chlorella vulgaris* have been demonstrated for the removal of organic pollutants and for their high value added products (Wang et al., 2019; Välitalo et al., 2017; Lv et al., 2018). In the present study, these four algal species were employed separately to remove ten frequently detected antibiotics, including sulfamerazine (SMR), sulfamethoxazole (SMX) and sulfamonomethoxine (SMM) from sulfonamide group; a pyrimidine inhibitor trimethoprim (TMP); clarithromycin (CLA), azithromycin (AZI), roxithromycin (ROX) from macrolide group; and lomefloxacin (LOM), levofloxacin (LEV) and flumequine (FLU) from fluoroquinolone antibiotic group, in a series of batch culture experiments. Special emphases were placed for: (1) understanding the removal mechanism and contribution via biodegradation, bioaccumulation, biosorption, or abiotic reaction, (2) elucidating the antibiotic dissipation kinetics, (3) identification of potential TPs by high resolution mass spectrometry and evaluation the potential risks of the TPs.

2. Materials and methods

2.1. Chemicals and reagents

High purity (≥ 98 %) certified reference standards of SMR, SMX, SMM, TMP, CLA, AZI, ROX, LOM, LEV and FLU were obtained from Sigma-Aldrich, GmbH Fluka and AccuStandard. Their CAS number, molecular formula, molecular weight, chemical structure, and other physico-chemical properties are given in Table S1 in the supplementary information (SI). HPLC grade methanol and formic acid were purchased from Merck. Milli-Q water system (Millipore) produced ultrapure water was used during sample processing and chromatography. Stock solutions for each antibiotic were prepared in methanol at 1000 μg ml^{-1}. Subsequently, the mix working standard solutions of 100.0, 10.0 and 1.0 μg ml^{-1} concentrations of all the antibiotics were prepared in methanol and stored at −20 °C, that were later used for the preparation of calibration regimes for chromatographic analysis and for spiking the batch cultures.

2.2. Microalgae culture conditions

Biodegradation assays were conducted in batch culture experiments by using FACHB-874, FACHB-271, FACHB-1475 and FACHB-24 strains

of *H. pluvialis*, *S. capricornutum*, *S. quadricauda and C. vulgaris*, respectively. The algal cultures were obtained from the Institute of Hydrobiology, Chinese Academy of Sciences. The microalgae cultures were multiplied and maintained on BG11 medium (Stanier et al., 1971) under autotrophic conditions at 25 ± 1 °C with fluorescent light illumination of 12 h light/12 h dark cycle (Fig. S1) in a controlled-growth chamber (PGX-350B, Safu Experimental Apparatus Technology, China).

2.3. Batch culture experiments

The biodegradation efficacy of antibiotics by microalgae was studied in batch culture experiments by using 250 ml pre-sterilized synthetic wastewater (Xu et al., 2014) (Table S2) in 500 ml Erlenmeyer flaks in triplicate. Microalgae cultures at mid-logarithmic growth phase in the BG11 medium were centrifuged with subsequent washing of the pellet with pre-sterilized synthetic wastewater for the inoculation purpose. The microalgae pellet was transferred to the batch culture flasks to maintain an initial microalgal population of 1×10^6 cells mL^{-1} for each algae. Control experiments were also conducted by using pre-sterilized synthetic wastewater without microalgae to elucidate the possible role of abiotic factors in the degradation of antibiotics. The microalgal batch cultures and the control experiments were spiked by adding 50, 125 and 250 µl of 100 µg ml^{-1} methanolic mix antibiotic standard solution to achieve 20, 50 and 100 µg L^{-1} initial concentrations, respectively. Set of flasks with and without microalgae were left un-spiked to serve as blank. The microalgae batch cultures were incubated at 25 ± 2 °C under 12 h light/12 h dark cycle fluorescent light (Fig. S1). The control flasks were kept in dark or the fluorescent light to indicate the hydrolysis or photolysis of antibiotics, respectively. The experiments were established over a period of 40 days. Aliquots (7.0 ml) were drawn from each treatment and control at 0, 5, 10, 15, 20, 30, and 40-day time interval to evaluate the microalgae growth, nutrient and antibiotic concentrations.

2.4. Measurement of algal growth

The algal cells were initially counted by hemocytometer at 400× magnification under microscope (Zeiss Axio Imager A_1), while, the absorbance of the microalgal culture was monitored at 680 nm using UV/Vis spectrophotometer (UV-5200, Metash, China). The concentration factor (CF) was then evaluated based on the measured absorbance against the counted cell numbers of each microalgal species according to the linear regression model (Burns et al., 2012). The CF values for *H. pluvialis*, *S. capricornutum*, *S. quadricauda* and *C. vulgaris* were 79.9, 213.3, 235.9 and 146.8, with R^2 values of 0.99, 0.95, 0.99 and 0.99, respectively. Algal growth in the batch culture was then evaluated based on Eq. 1 by monitoring the absorbance at 680 nm.

$$n = \frac{(OD \times CF \times 400 \times 10{,}000)}{80} \quad (1)$$

Where, n is the number of algal cells (cells ml^{-1}), OD is absorbance at 680 nm, and CF is the concentration factor.

2.5. Analysis of nutrients and antibiotics

The determination of PO_4^{3-}-P and NO_3^--N was carried out by microplate technique (Hernández-López and Vargas-Albores, 2003). Detailed description of the microplate technique is given in Text S1.

The dissolved, bioadsorbed, and bioaccumulated antibiotic residues were analyzed in three steps. (1) For the dissolved antibiotics, 6.0 ml sample was centrifuged at 4500 rpm for 5 min and the supernatant (4.0 ml) was frozen at −20 °C, subsequently, freeze-dried with Labconco freeze-dryer (FreeZone 6 L Benchtop, USA), reconstituted in 1.0 ml methanol and passed through a 0.22 µm membrane filter (Anpel Laboratory Technologies, Shanghai) in LC-vial, and stored at −20 °C prior to further analysis. (2) The pellet produced by centrifugation of 6.0 ml sample described above, was dispersed and vortex mixed in 6.0 ml Milli-Q water to wash the adsorbed antibiotics from algal cells (Xiong et al., 2016). The mixture was centrifuged at 4500 rpm for 5 min and 5.0 ml of supernatant was freeze dried, reconstituted in 1.0 ml methanol, filtrated, and stored at −20 °C for the determination of bioadsorbed antibiotics. (3) For the bioaccumulated antibiotics fraction, the surface washed algal cells in the pellet were mixed with 6.0 ml of dichloromethane:methanol (1:2 v/v) and sonicated for 1 h (40 kHz, 2.2 Kw) to facilitate the cell lysis and the release of cell sap (Xiong et al., 2016). Subsequently, the mixture was centrifuged at 4500 rpm for 10 min. The supernatant was retrieved and concentrated to near dryness under gentle nitrogen stream and reconstituted in 1.0 mL methanol and filtrated into LC-vial.

The quantitative determination of antibiotics was carried out by using liquid chromatography with triple quadrupole mass spectrometry (LC-QqQ-MS, ABI 3200 QTRAP, USA) by multiple reaction monitoring (MRM) in positive electrospray ionization (+ESI) mode (Table S3). The chromatographic separation of the antibiotics was achieved by a Kinetex 2.6 µm C18 column (100 mm × 2.1 mm, Phenomenex, USA) on Shimadzu LC system (LC-20A, Shimadzu, Japan) by using binary gradient mobile phase constituting ultrapure water buffered with 0.1 % formic acid (A) and HPLC grade methanol (B). The ratio of B was ramped from 5% at 0.01 min to 80% at 0.5 min, 100% from 1.5 to 3.0 minutes, and 5% at 3.1 min at a total flow rate of 0.8 mL min^{-1} and total runtime of 4.5 min.

2.6. Identification of the TPs

The TPs were monitored in the microalgae batch cultures spiked at 20 and 100 µg L^{-1} antibiotic concentrations at 0, 5, 15 and 30 sampling days. TPs in 100 µg L^{-1} spiking level batch culture were monitored in the same samples already drawn for the determination of dissolved antibiotics (descibed in section 2.5). In view of the expected low TP concentrations in 20 µg L^{-1} batch cultures, an aliquot (10 ml) was drawn from the batch culture, freeze dried, concentrated in 1.00 ml methanol, purified by 0.22 µm syringue filter and stored in −20 °C freezer.

The samples were analyzed by UPLC-ESI-HRMS containing an ACQUITY UPLC I-Class System (Aquity, UK) coupled with Q-ToF (H-Class-Xevo G2-XS, Waters, UK) in +ESI mode with data collection by MS^E methodology. The chromatographic separation was achieved by a Kinetex 2.6 µm C18 column (100 mm × 2.1 mm, Phenomenex, USA) by using binary gradient mobile phase constituting ultrapure water buffered with 0.1 % formic acid (A) and HPLC grade methanol (B). The concentration of B was ramped from 5% at 0.01 min to 95% at 8 min, 95% from 8.0 to 10.01 min, and 5% at 10.01 min at a total flow rate of 0.3 mL min^{-1} and total runtime of 12.0 min. The injection volume was 5.0 µL and the mass accuracy was maintained by employing lockspray function with leucine-enkephalin. The capillary and lockspray capillary voltages were set at 3.2 kV and 1.20 kV, respectively. The corona, cone, sampling cone and extraction cone voltages were set at 3.0 kV, 40 V, 25 V and 4 V, respectively. The desolvation and source temperatures were set at 450 °C and 100 °C, respectively. Nitrogen (20 ± 2 °C; 10 psi) at a flow rate of 50 and 700 L h^{-1} was used as cone and desolvation gases, respectively. MS was conducted with low collision energy (6 V), while, MS/MS was conducted at higher ramped range of collision energy from 20 to 30 V to induce fragmentation mass range from 100 to 1000 *m/z*. Data acquisition for the parent and subsequent fragmentation ions was simultaneously done by both MS and MS/MS functions by using 0.5 s scan time and 14 ms inter-scan delay. All data collection was performed in sensitivity mode (Resolution = 30,000–40,000).

Post-acquisition analyses were performed with MetaboLynx™ XS (v4.1) Application Manager (Waters Corp., Milford, MA, USA) that uses a broad list of probable biotransformation reactions in combination with the basic composition of the inserted molecules in a method file, to generate a sequence of extracted ion chromatograms. The identification

of TPs was carried out by employing the suspect screening approach. The potential TPs were proposed on the basis of published research, prediction system by EAWAG-Biodegradation/Biocatalysis Database (EAWAG-BBD), and built-in program of MetaboLynx™ XS software, and subsequently, confirmed by using MetaboLynx™ XS software with the criteria of error $\leq \pm 5$ mg L^{-1}. The metabolized sample data was compared with the control samples and the unique peaks appearing only in the experimental samples were considered as possible expected metabolites.

2.7. Data processing and statistical analysis

The dissipation percentage (P_d) of antibiotics by the biotic and abiotic degradation was calculated by using Eq. 2, while, the biodegradation percentage (P_b) of the antibiotics induced by the microalgal species was calculated by using Eq. 3 (Xiong et al., 2017b):

$$P_d(\%) = (A_t - A_r - A_d - A_c)\frac{100}{A_t} \quad (2)$$

$$P_b(\%) = (A_t - A_r - A_d - A_a - A_c)\frac{100}{A_t} \quad (3)$$

Where, A_t is the initial concentration of each compound added to the medium, A_r is the residual amount of each antibiotic in the medium, A_d is the amount of each antibiotic bioadsorbed by the microalgal cell surface, A_a is the amount of each antibiotic removed by abiotic processes, and A_c is the amount of each antibiotic bioaccumulated in the microalgal cells.

The antibiotics dissipation kinetics was studied based on the overall

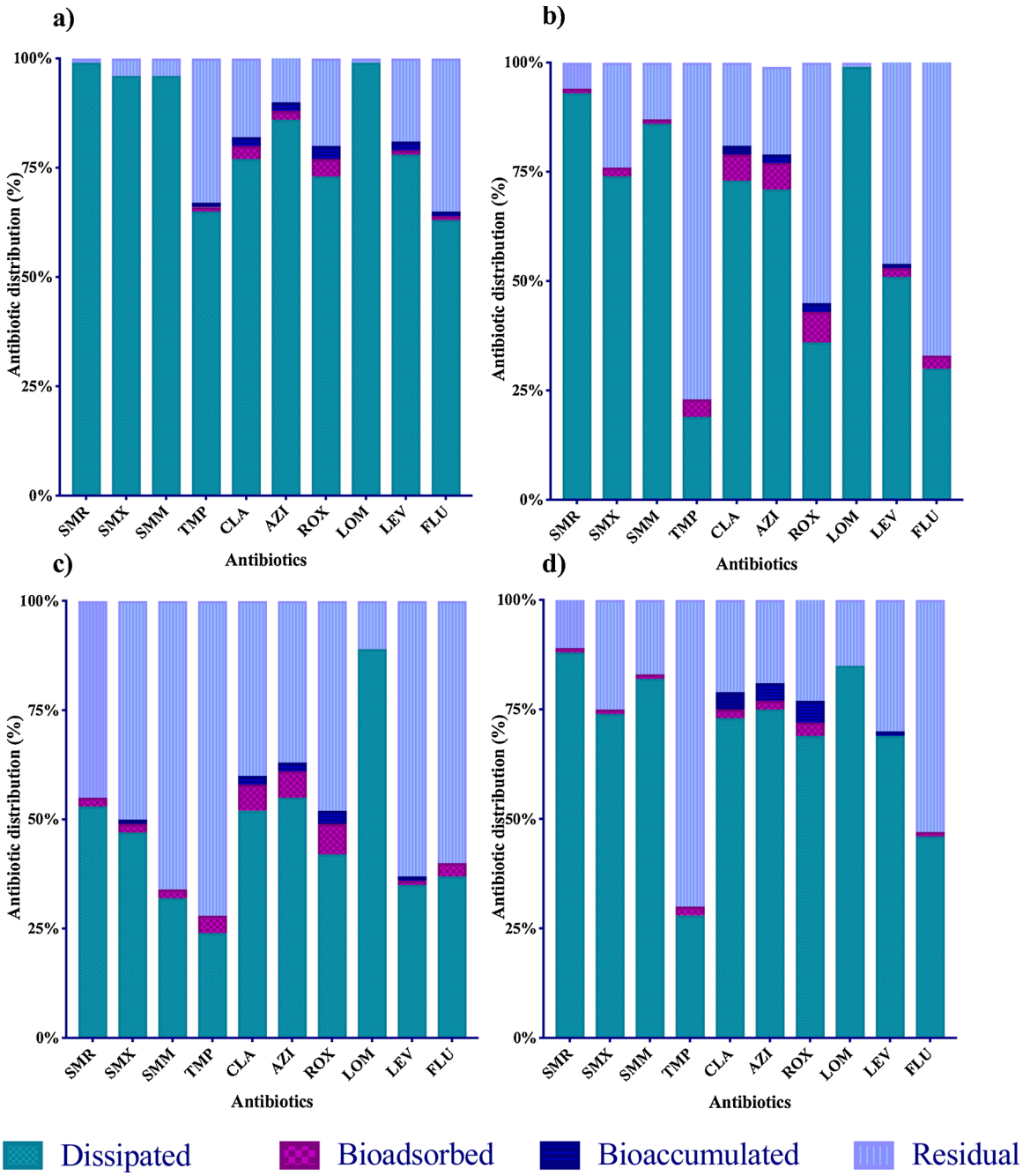

Fig. 1. Mean relative distribution (%) of antibiotics as dissipated, bioadsorbed, bioaccumulated and residual in batch cultures of (a) *H. pluvialis*, (b) *S. capricornutum*, (c) *S. quadricauda*, and (d) *C. vulgaris* spiked at 20 and 100 μg L^{-1} concentration levels of antibiotics.

disappearance of the antibiotics by fitting the temporal residual concentration to a pseudo-first-order model (Eq. 4)

$$-\ ln\left(\frac{C_t}{C_0}\right) = k \times t \tag{4}$$

Where, C_0 and C_t are the antibiotic concentrations at initial "0" and time "t" intervals, respectively. The degradation rate constant (k) and half-life ($t_{1/2}$) were determined by Eqs. 5 and 6, respectively.

$$k = -\ ln\left(\frac{C_t}{C_0}\right)/t \tag{5}$$

$$t_{1/2} = \frac{ln\ (2)}{k} \tag{6}$$

The relationship between the algal cell growth and the removal of antibiotics and nutrients was characterized as the coefficients of Monod's model (Jacques, 1949) which is a mathematical analogue of Michaelis-Menten kinetic model given as Eq. (7).

$$\mu = \mu_{max} \times \frac{S}{k_s + S} \tag{7}$$

Where, μ (h^{-1}) is the specific growth rate, μ_{max} (h^{-1}) is the maximum specific growth rate, S (μg L^{-1}) is the substrate concentration and k_s (μg L^{-1}) is the half-saturation constant defined as the concentration of the growth limiting substance (nutrients and antibiotics). The specific growth rate (μ) of algae is one-half of the maximum specific growth rate (μ_{max}). The specific growth rate (μ) of algae was calculated for the exponential phase of growth curves produced for 20, 50 and 100 μg L^{-1} initial concentration of the antibiotics by using Eq. 8.

$$\mu = \frac{ln(C_t) - ln\ (C_0)}{t - t_0} \tag{8}$$

Where, C_t and C_0 are the concentrations of the substrate at final time t and initial time t_0 of the exponential phase of the growth curve at each concentration. Monod coefficients, K_s and μ_{max} were determined by using the Lineweaver-Burk plot of reciprocals of the specific growth rates ($1/\mu$) determined for respective substrate initial concentrations ($1/S$) as shown in Eq. 9.

$$\frac{1}{\mu} = \frac{K_s}{\mu_{max}} \times \frac{1}{S} + \frac{1}{\mu_{max}} \tag{9}$$

The appropriateness of the model was determined by regression coefficients (R^2), and root mean square error (RMSE). Subsequently, the divisions of algal cells per day (D_d) and the doubling time were calculated by Eqs. 10 and 11, respectively.

$$Divisions\ per\ day\ (D_d) = \frac{\mu_{max}}{ln\ (2)} \tag{10}$$

$$Doubling\ time = \frac{1}{D_d} \tag{11}$$

3. Results and discussions

3.1. Growth of algae

The natural logarithmic growth of *H. pluvialis*, *S. capricornutum*, *S. quadricauda and C. vulgaris* is given in Fig. S2. The growth pattern of the four algae at different antibiotic concentrations was almost consistent, where, the lag phase was absent and the exponential growth of algae was mostly observed between 0–5 days, with the exception of *S. capricornutum* in the un-spiked batch. The absence of lag phase in this study was probably due the reason that established algal cultures grown under similar conditions of the experimentation were used (de Morais and Costa, 2007). Generally, each alga exhibited a unique growth rate under different antibiotic concentrations. *H. pluvialis* showed a significant increase in the growth rate at higher antibiotic concentration compared to growth in control (un-spiked medium) (Fig. S2), indicating the utilization of organic compounds as nutritional sources (Santos Escapa et al., 2017). Similar pattern was observed for *C. vulgaris*. In case of *S. quadricauda* and *S. capricornutum*, an increased growth was observed at 20 μg L^{-1} levels, however, at the higher concentration levels, the growth rate decreased. This might be due to the inhibitory effect of one or more of the antibiotics at higher concentration levels.

3.2. Bioadsorption and bioaccumulation of antibiotics

The mean partitioning of the antibiotics as bioadsorbed and bioaccumulated fraction, the quantity dissipated and left over as residues in synthetic wastewater spiked at 20 and 100 μg L^{-1} concentrations in batch cultures of different algal species after 40 days are given in Fig. 1. The relative partitioning values for the individual spiking levels of 20 and 100 μg L^{-1} are presented in Tables S4 and S5, respectively. Generally, a similar pattern of bioadsorption and bioaccumulation of the antibiotics was observed among different algal species, however, variation existed among different antibiotic groups. Bioaccumulation of sulfonamides was non-existant for all the four algae. Likewise, relatively low bioadsorption (1–4%) of sulfonamides was observed in *S. capricornutum, S. quadricauda* and *C. vulgaris*. Among the fluoroquinolone antibiotics, no bioabsorption or bioaccumulation was observed for LOM, while, the bioadsorption ranged from 1–3% and bioaccumulation of 1–2% of LEV and FLU antibiotics for the four algae. Macrolide antibiotics (CLA, AZI and ROX) showed a relatively higher tendency of both bioadsoprtion and bioaccumulation compared to other antibiotic groups. Variations in the bioadsoprtion and bioaccumulation of macrolides also varied among the algal species. Bioadsorption of macrolides ranged between 2–4% in *H. pluvialis* and *C. vulgaris*, while, 6–7% in *S. capricornutum* and *S. quadricauda*. Bioaccumulation of the three macrolide antibiotics was consistent (2–3%) for *H. pluvialis, S. capricornutum* and *S. quadricauda*, while, relatively higher (4–5%) in *C. vulgaris*. Bioadsorption and bioaccumulation of the organic compounds depend upon the hydrophobicity of a compound that is indicated by the *n*-octanol water partitioning coefficient log Kow (Arpin-Pont et al., 2016). The compounds with higher log Kow generally have higher values of bioconcentration factor. Therefore, the sulfonamides and fluoroquinolones with log Kow values 0.14–0.91 and -0.3–1.6 (Table S1), showed lower bioadsorption and bioaccumulation tendencies. In contrary, the log Kow of the macrolides ranged between 3.0–4.02 indicating higher hydrophobicity and a relatively higher tendency of bioadsorption and bioaccumulation were observed. In short, bioadsorption and bioaccumulation had minor contributions on the total removal of the antibiotics in this work.

3.3. Abiotic and biotic dissipation

The abiotic control experiments without algae under illuminated or dark conditions indicated photodegradation (Fig. S3) and hydrolysis (Fig. S4) of antibiotics, respectively. Among the three spiked levels, relatively higher removal of antibiotics was observed for 20 μg L^{-1} compared to the higher spiked levels. The mean removal of antibiotics by photodegradation in 20, 50 and 100 μg L^{-1} spiked concentrations over 40 days of incubation showed 5–8 % removal for the sulfonamides (SMR, SMX and SMM), 24–27 % for the macrolides (CLA, AZI, AZI) and 14 % for that of LEV and FLU (Fig. S5). Since, the illuminated control experiment was conducted in the absence of algal biomass, the self-shading phenomenon in the algal cultures may result in reduction in the photodegradation due to the poor light penetration in the presence of growing algal population (González-Camejo et al., 2019). Therefore, in view of the low effect of photodegradation in the illuminated control and the anticipated lower effect due to the self-shading in the batch culture experiments, the antibiotic removal was mainly ascribed to

biotic dissipation with minor contributions from bioadsorption, bioaccumulation, and abiotic factors. However, LOM was an exception, where, more than 98 % dissipation was caused by photolysis over 40-days incubation period (Fig S3). Hence, the removal of LOM was attributed to the abiotic photodegradation.

The mean removal of antibiotics for 20, 50 and 100 μg L^{-1} initial concentrations in the four batch cultures is presented in Fig. S6. Microalgae-specific pattern of antibiotic removal were observed. *H. pluvialis* was the most efficient algal specie with antibiotic removal efficiencies ranging between 42–100% with median value of 93 %, followed by *S. capricornutum, C. vulgaris and S. quadricauda,* with the median removal efficiencies of 82 %, 78 %, and 47 %; ranging between 9–99%, 23–98%, and 10–100% for different antibiotics, respectively. The residual antibiotic concentration (C_t/C_0) versus time (days) plots for the three initial antibiotic concentrations in batch cultures of *H. pluvialis*, *S. capricornutum*, *S. quadricauda,* and *C. vulgaris* are presented in Figs. 2 and S7–S9, respectively. The removal of antibiotics in the microalgae batch cultures followed the pseudo-first-order kinetics. The half-lives of the antibiotics were shortest in *H. pluvialis* batch culture, ranging between 2.4–4.2 days for the sulfonamides, followed by 3.7–9.4 days for macrolides, 2.1–12.2 days for fluoroquinolones, and 8.0–14.8 days for pyrimidine inhibitor TMP (Table 1). Previous studies have also showed a good performance of *H. pluvialis* for the removal of organic pollutants from wastewater including metoprolol (Lv et al., 2018) and estrogens (Wang et al., 2019).

The removal efficiencies were non-significantly different across different initial concentrations for all the antibiotics with *p*-value ranging from 0.12 for LEV to 0.92 for SMX at $\alpha = 0.05$. Across all the three initial concentrations, the average removal efficiencies of SMR, SMX, and SMM of sulfonamide group were 84 %, 74 %, and 75 %, respectively, while, it was only 37 % for TMP. Among the macrolide antibiotics, CLA, ROX, and AZI underwent 76 %, 63 %, and 78 % removal over 40-days of incubation. Similar removal efficiencies were reported for CLA and ROX in wastewater influent by four microalgae including

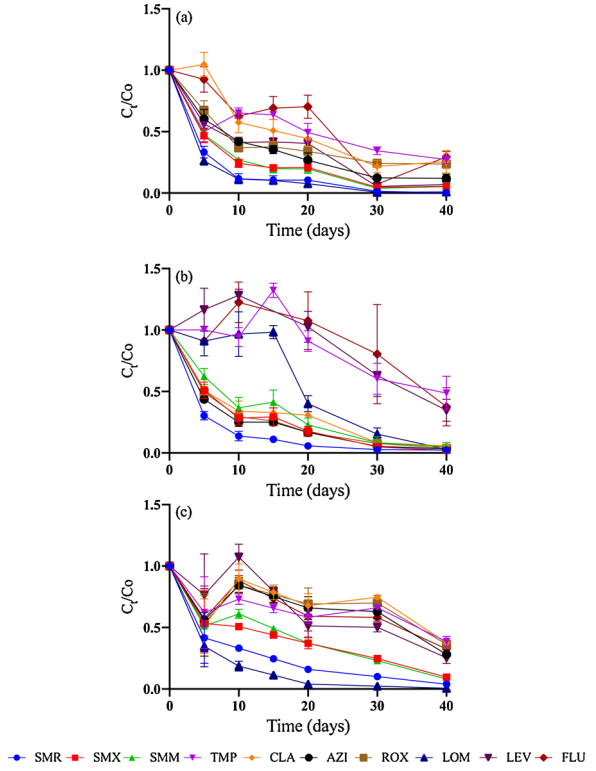

Fig. 2. Antibiotic dissipation (C_t/C_0) in *H. pluvialis* at (a) 20, (b) 50 and (c) 100 μg L^{-1} initial concentration in batch cultures. Error bars represent ± standard error of mean.

C. vulgaris (Zhou et al., 2014). Among the fluoroquinolones, the highest removal efficiency (93 %) was achieved for the photosensitive LOM. However, relatively lower removal was observed for LEV (60 %) and FLU (46 %). In a previous study, low removal of LEV (4 %) by *S. obliquus* was reported in wastewater after 11-days of incubation (Xiong et al., 2017b).

3.4. Nutrient removal

The initial NO_3^--N and PO_4^{3-}-P concentrations in the batch cultures were 12.04 and 5.89 mg L^{-1}, respectively. The removal of NO_3^--N and PO_4^{3-}-P in *H. pluvialis, S. capricornutum, S. quadricauda* and *C. vulgaris* batch cultures at 20, 50 and 100 μg L^{-1} mixed antibiotics spiked concentrations are given in Fig. 3. The nutrient removal efficiencies varied among the algal species as well as the antibiotic spike concentrations. The removal efficiencies of NO_3^--N were almost similar at 20 μg L^{-1} spike level for the four batch cultures. However, significant variations were observed among the batch cultures at 50 and 100 μg L^{-1} antibiotic concentrations. The NO_3^--N removal was significantly higher (97 %) at 20 μg L^{-1} than at 50 and 100 μg L^{-1} concentations in *S. quadricauda*, corresponding to the growth rate of algae at different concentrations (Fig. S2). The PO_4^{3-}-P removal in *S. capricornutum* (76–78%) and *S. quadricauda* (94–97%) was almost similar for the three antibiotic concentations, while, it significantly varied among the antibiotic spiking levels for both *H. pluvialis* and *C. vulgaris*. In *H. pluvialis* batch culture, reletively lower removal of PO_4^{3-}-P (68 %) was observed at 20 μg L^{-1} followed by 74 % and 85 % at 50 μg L^{-1} and 100 μg L^{-1} spiking levels, respectively. In contrary, the highest PO_4^{3-}-P removal (96 %) was recorded at 20 μg L^{-1}, followed by 85 % and 77 % at 50 μg L^{-1} and 100 μg L^{-1} spiking levels, respectively for *C. vulgaris*. Depletion of the nutrients was relatively faster in *H. pluvialis* and *C. vulgaris* than *S. capricornutum* and *S. quadricauda* batch cultures (Fig. S10).

3.5. Monod kinetics

In the present study, Monod kinetics was applied to investigate the dissipation of antibiotics and nutrients by the algae. Single substrate utilization Monod model was used instead of a mixed substrate model with the assumption that the antibiotics and nutrients behave independent of each other. The parameters of Monod kinetics viz. maximum specific growth (μ_{max}) and half-saturation constant (k_s) are presented in Table 2. The calculated parameters were validated by RMSE and R^2 for the measured and the predicted specific growth rates. The R^2 values ranged from 0.41 – 1.0, 0.64 – 1.0, 0.41 – 0.69 and 0.70 – 1.0 for *H. pluvialis, S. capricornutum, S. quadricauda and C. vulgaris*, respectively. Generally, the lower R^2 values for Monod's model suggest a more profound effect of substrate or product inhibition on the growth of biodegrading organism (Dutta et al., 2014). The μ_{max} varied among algal species as well as with respect to different antibiotics and nutrients. Relatively higher μ_{max} was obeserved for *C. vulgaris* with median μ_{max} value of 0.31 day^{-1} ranging from 0.30 – 0.31 day^{-1} followed by *H. pluvialis* with median μ_{max} value of 0.24 day^{-1} ranging from 0.05 – 0.65 day^{-1}, *S. quadricauda* with median μ_{max} value of 0.21 day^{-1} ranging from 0.20 to 1.29 day^{-1}, and *S. capricornutum* with median μ_{max} value of 0.08 day^{-1} ranging from 0.05 – 0.13 day^{-1}. Similar specific growth rates for these microalgae were reported in previous studies (de Morais and Costa, 2007; Goswami and Kalita, 2011; Cheng et al., 2016).

Half saturation constant (k_s) is an important parameter that represents the concentration at which half of the maximum specific growth rate ($\mu_{max}/2$) is reached. It is also referred to as the affinity constant of the substrate, where, the compounds with low k_s values indicate higher affinity, while, those with higher k_s indicate low affinity (Kong et al., 2018) or inefficiency of the algae for biodegradation (Mulder and Hendriks, 2014). In the present study, lowest k_s values for

Table 1
Pseudo-first-order kinetic parameters, rate constant (k: d^{-1}), half-lives ($t_{1/2}$: d), determination coefficient (R^2).

Antibiotics	Concentrations (μg L^{-1})	*H. pluvialis*			*S. capricornutum*			*S. quadricauda*			*C. vulgaris*		
		k	$t_{1/2}$	R^2	k	$t_{1/2}$	R^2	k	$T_{1/2}$	R^2	k	$T_{1/2}$	R^2
SMR	20	0.137 ± 0.029	2.42 ± 0.52	0.88	0.122 ± 0.011	2.51 ± 0.25	0.92	0.004 ± 0.004	30.0 ± 3.39	0.60	0.025 ± 0.013	4.85 ± 0.33	0.94
	50	0.107 ± 0.002	2.82 ± 0.06	0.95	0.116 ± 0.014	2.67 ± 0.31	0.94	0.024 ± 0.007	10.41 ± 1.24	0.86	0.035 ± 0.005	4.89 ± 0.56	0.87
	100	0.083 ± 0.001	3.67 ± 0.04	0.93	0.109 ± 0.013	2.84 ± 0.33	0.92	0.035 ± 0.035	25.0 ± 2.51	0.09	0.076 ± 0.007	4.04 ± 0.35	0.91
SMX	20	0.087 ± 0.002	3.45 ± 0.08	0.91	0.14 ± 0.047	2.61 ± 0.71	0.95	0.024 ± 0.018	3.06 ± 1.56	0.61	0.05 ± 0.013	6.01 ± 0.48	0.93
	50	0.102 ± 0.015	3.13 ± 0.55	0.95	0.059 ± 0.003	5.15 ± 0.27	0.82	0.024 ± 0.006	9.05 ± 0.91	0.66	0.039 ± 0.004	6.58 ± 1.68	0.69
	100	0.073 ± 0.004	4.26 ± 0.29	0.86	0.034 ± 0.012	12.83 ± 5.9	0.90	0.091 ± 0.04	3.08 ± 0.77	0.85	0.032 ± 0.006	10.04 ± 2.12	0.87
SMM	20	0.095 ± 0.003	3.16 ± 0.1	0.94	0.057 ± 0.007	5.47 ± 0.69	0.82	0.038 ± 0.013	5.82 ± 0.15	0.84	0.043 ± 0.007	5.35 ± 0.54	0.93
	50	0.087 ± 0.017	3.8 ± 0.87	0.95	0.094 ± 0.02	3.48 ± 0.63	0.85	0.061 ± 0.042	7.98 ± 3.02	0.79	0.035 ± 0.005	4.41 ± 0.96	0.87
	100	0.089 ± 0.009	3.66 ± 0.46	0.90	0.05 ± 0.006	6.20 ± 0.72	0.90	0.064 ± 0.03	6.03 ± 2.51	0.87	0.038 ± 0.006	8.31 ± 1.24	0.88
TMP	20	0.027 ± 0.001	11.31 ± 0.31	0.76	0.02 ± 0.003	15.67 ± 2.45	0.65	0.033 ± 0.011	6.78 ± 0.12	0.69	0.04 ± 0.005	17.67 ± 6.13	0.32
	50	0.026 ± 0.007	14.82 ± 5.7	0.67	0.005 ± 0.002	69.03 ± 1.03	0.54	0.009 ± 0.005	77.67 ± 12.5	0.35	0.035 ± 0.005	32.43 ± 16.31	0.44
	100	0.037 ± 0	8.08 ± 0.06	0.98	0.003 ± 0.003	14.60 ± 2.43	0.06	0.03 ± 0.03	4.06 ± 2.58	0.54	0.012 ± 0.006	11.39 ± 5.69	0.54
CLA	20	0.049 ± 0.006	6.31 ± 0.73	0.80	0.061 ± 0.003	4.93 ± 0.21	0.92	0.046 ± 0.017	4.61 ± 0.17	0.88	0.049 ± 0.012	2.75 ± 0.38	0.92
	50	0.071 ± 0.008	4.36 ± 0.47	0.93	0.054 ± 0.005	5.68 ± 0.46	0.83	0.019 ± 0.004	14.46 ± 1.51	0.85	0.031 ± 0.008	2.23 ± 0.28	0.95
	100	0.053 ± 0.004	6.02 ± 0.56	0.89	0.033 ± 0.01	11.87 ± 1.88	0.75	0.034 ± 0.016	28.8 ± 3.25	0.47	0.027 ± 0.011	14.51 ± 4.16	0.75
AZI	20	0.056 ± 0.006	5.54 ± 0.56	0.89	0.069 ± 0.003	4.36 ± 0.16	0.94	0.064 ± 0.028	3.34 ± 0.44	0.88	0.059 ± 0.021	2.59 ± 0.35	0.93
	50	0.083 ± 0.009	3.73 ± 0.43	0.95	0.062 ± 0.005	4.95 ± 0.37	0.89	0.025 ± 0.007	9.63 ± 0.4	0.91	0.035 ± 0.005	3.05 ± 0.33	0.82
	100	0.057 ± 0.004	5.59 ± 0.48	0.83	0.023 ± 0.006	14.57 ± 3.29	0.80	0.015 ± 0.01	81.3 ± 3.41	0.21	0.026 ± 0.008	13.69 ± 3.72	0.84
ROX	20	0.033 ± 0.003	9.36 ± 0.83	0.79	0.02 ± 0.002	14.96 ± 1.38	0.75	0.036 ± 0.012	6.42 ± 0.21	0.79	0.04 ± 0.005	4.07 ± 0.39	0.94
	50	0.079 ± 0.005	3.86 ± 0.24	0.97	0.023 ± 0.004	13.72 ± 2.22	0.78	0.022 ± 0.005	11.79 ± 0.88	0.73	0.033 ± 0.006	7.84 ± 3.28	0.65
	100	0.042 ± 0.004	7.74 ± 1.05	0.74	0.004 ± 0.001	175.23 ± 7.15	0.47	0.005 ± 0.001	112.3 ± 5.77	0.10	0.021 ± 0.001	14.47 ± 0.55	0.70
LOM	20	0.103 ± 0.008	2.97 ± 0.26	0.93	0.114 ± 0.011	2.69 ± 0.28	0.91	0.043 ± 0.016	5.12 ± 0.32	0.81	0.046 ± 0.009	4.99 ± 0.5	0.93
	50	0.078 ± 0.008	3.95 ± 0.44	0.84	0.145 ± 0.039	2.36 ± 0.54	0.96	0.033 ± 0.011	7.4 ± 0.68	0.79	0.038 ± 0.004	3.95 ± 0.54	0.89
	100	0.146 ± 0.01	2.17 ± 0.19	0.94	0.182 ± 0.041	1.89 ± 0.54	0.91	0.32 ± 0.055	0.86 ± 0.05	0.91	0.116 ± 0.016	2.70 ± 0.35	0.96
LEV	20	0.054 ± 0.005	5.72 ± 0.57	0.80	0.047 ± 0.003	6.52 ± 0.42	0.87	0.03 ± 0.009	7.75 ± 0.62	0.79	0.039 ± 0.004	6.92 ± 1.35	0.88
	50	0.034 ± 0.008	10.08 ± 2.75	0.71	0.216 ± 0.241	44.59 ± 6.99	0.45	0.021 ± 0.005	13.85 ± 1.96	0.37	0.031 ± 0.008	9.84 ± 2.56	0.83
	100	0.088 ± 0.023	4.98 ± 1.84	0.93	0.071 ± 0.02	4.82 ± 1.07	0.90	0.106 ± 0.059	3.83 ± 1.88	0.79	0.042 ± 0.009	8.29 ± 2.37	0.83
FLU	20	0.031 ± 0.004	10.22 ± 1.58	0.83	0.025 ± 0.004	12.79 ± 2.61	0.83	0.012 ± 0.007	8.18 ± 4.13	0.54	0.034 ± 0.006	13.36 ± 4.29	0.66
	50	0.017 ± 0.009	12.20 ± 0.38	0.59	0.005 ± 0.002	66.34 ± 5.8	0.36	0.011 ± 0.001	22.77 ± 5.54	0.42	0.033 ± 0.006	0	0
	100	0.038 ± 0.004	8.51 ± 1.13	0.87	0.031 ± 0.04	54.11 ± 7.12	0.41	0.01 ± 0.044	4.10 ± 0.78	0.64	0.054 ± 0.03	9.20 ± 3.38	0.84

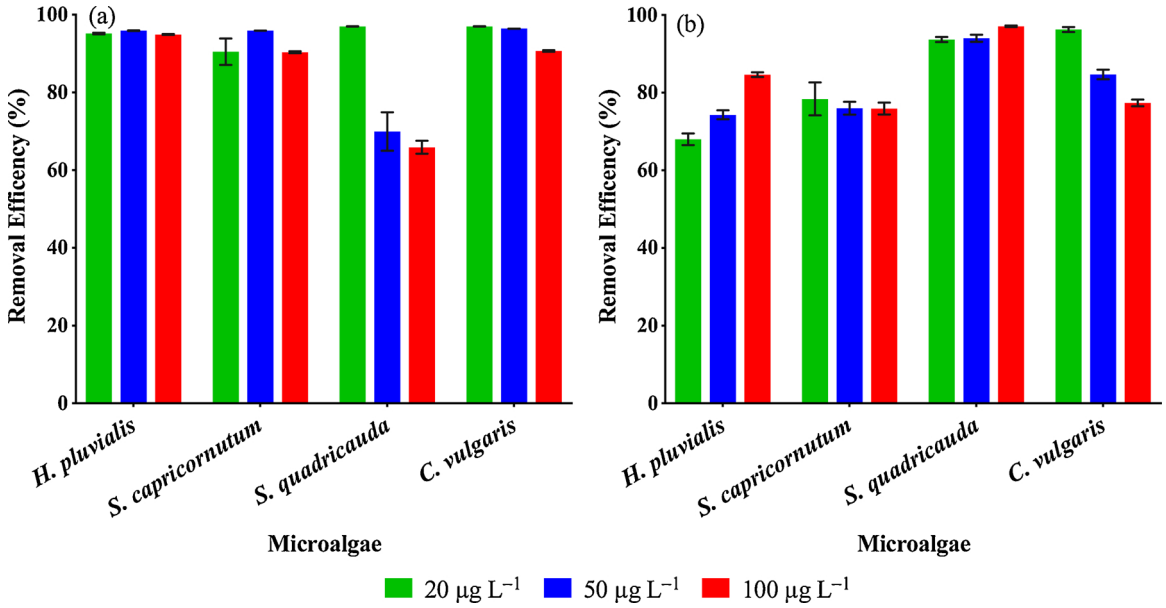

Fig. 3. The removal of (a) NO_3^--N and (b) PO_4^--P at different antibiotic spike concentrations in the batch cultures of *H. pluvialis, S. capricornutum, S. quadricauda* and *C. vulgaris*. Error bars represent ± standard error of mean.

the antibiotics and nutrients were obtained for *S. capricornutum* that ranged from –0.38 to –15.36 µg L^{-1} with an average value of –9.93 µg L^{-1}. According to Eppley et al., there is no physical interpretation of the negative value of k_s (Eppley et al., 1969), however, Converti et al., attributed the negative values of k_s to maximum degradation rate (Converti et al., 1999). The slope (k) of the pseudo-first-order degradation kinetic for the antibiotics (Table 1) also support the later argument. Value of k in *S. capricornutum* batch culture that ranged from 0.02 – 0.14 day^{-1} excluding TMP (k = 0.005) also indicated relatively higher rates of degradation than *H. pluvialis, S. quadricauda* and *C. vulgaris*, where, the values of k ranged from 0.03 – 0.11 day^{-1}, 0.01 – 0.06 day^{-1} and 0.028 – 0.037 day^{-1}, respectively. *S. capricornutum* showed the nutritional choice of the order CLA > FLU > ROX > TRI > AZI > LEV > SMM > SMX > SMR for the antibiotics with negative k_s values. This was followed by *C. vulgaris* batch culture, where, the k_s values ranged from 0.07 – 0.36 µg L^{-1}. *C. vulgaris* showed the affinities of the order LEV > ROX > TRI > SMX > SMR > FLU > SMM > AZI > CLA for the antibiotics. Considerably higher values of k_s were obtained for antibiotics and nutrients in *H. pluvialis* and *S. quadricauda* batch cultures that ranged from 2.79 – 103.7 µg L^{-1} and 8.53–145.4 µg L^{-1}, respectively. These results indicated very low affinity of *H. pluvialis* and *S. quadricauda* for the antibiotics. The affinities were of the order SMR > SMX > AZI > TRI > SMM > LEV > FLU > CLA > ROX for *H. pluvialis* and SMX > SMM > SMR > AZI > LEV > ROX > TRI > CLA > FLU for *S. quadricauda*.

The use of μ_{max}/k_s ratio, which take into account the variations in μ_{max} on the interpretation of k_s, can better explain the competition among the limiting nutrients for the growth of biodegradaing organisms by depicting the rate of biodegradation (Fareed et al., 2017). The higher μ_{max}/k_s ratio indicates higher growth rate at lower concentration level emphasizing a comparative advantage of an organism for biodegradation of a compound, while, the lower μ_{max}/k_s ratio indicates the slow growth rate of an organism at higher concentration level of a compound, suggesting, disadvantage for biodegradation and inefficient removal efficiency of the organism. The μ_{max}/k_s ratios are presented in Table 2. Highest values of μ_{max}/k_s ratio were obtained for *C. vulgaris* for almost all the antibiotics as well as for the NO_3^--N and PO_4^{3-}-P nutrients. The μ_{max}/k_s ratio ranged from 0.88 for CLA with slowest degradation rate to 4.49 for LEV with highest rate of degradation by *C. vulgaris*. These results indicated the ability of *C. vulgaris* to simultaneously utilize homologous substances as a nutritional sources. Kovárová-Kovar and Egli reviewed such resource utilization by the organisms, where, the underlying principle of kinetics was described as utlization of mixtures of carbon sources (Kovárová-Kovar and Egli, 1998). The removal efficiency for NO_3^--N and PO_4^{3-}-P was almost similar with μ_{max}/k_s ratios of 1.14 and 1.20, respectively. *C. vulgaris* was followed by *H. pluvialis* with μ_{max}/k_s ratios ranging from 0.007 – 0.084 for antibiotics with lowest rate of degradation for AZI and highest for SMR. However, *H. pluvialis* achieved highest antibiotic removal (42–100%) over a period of 40 days of incubation (Section 3.2). *H. pluvialis* showed poor efficiency for the removal of macrolides compared with other antibiotics used in this study. Nutrient removal efficiency of *H. pluvialis* also varied, where, relatively higher removal efficiency of NO_3^--N was observed compared to PO_4^{3-}-P with μ_{max}/k_s ratios of 0.093 and 0.019, respectively. These results indicated a selective antibiotic removal efficiency of *H. pluvialis*. Similarly, consistently low and selective removal efficiency was also observed for *S. quadricauda*. Relatively higher removal rates were observed for the sulfonamides, compared to fluoroquinolone and macrolide antibiotics. Considerably large variations in the removal efficiency of NO_3^--N and PO_4^{3-}-P was also observed. The removal efficiency of the PO_4^{3-}-P by *S. quadricauda* was approximately two times higher than the NO_3^--N. *S. capricornutum* produced negative μ_{max}/k_s ratios indicating very slow rates of biodegradation and removal efficiencies. Both group-specific and compound-specific nutritional preferences and removal efficiencies were observed for different algae. *S. capricornutum* and *C. vulgaris* indicated more affinity for the macrolides and fluoroquinolones than sulfonamides, while, *H. pluvialis* and *S. quadiricauda* showed relatively higher preference for sulfonamides than the other antibiotic groups.

3.6. Identification of TPs

A total of 10 TPs were identified from algal batch cultures. Their retention time, detected m/z, proposed molecular formula, theoretical m/z, error (ppm), and proposed structures are listed in Table S6. Intensities of TPs by Q/ToF-MS in different microalgal cultures and at different sampling times are given in Table S7.

Eight metabolites viz. TP306-1, TP306-2, TP290-1, TP290-2, TP282, TP184, TP168 and TP154 were detected and identified as TPs of TMP in

Table 2
Maximum specific growth rate (μ_{max}) and half saturation constant (K_s) parameters for Monod function and doubling time of different algae in relation to different antibiotics and nutrients. Model fitness criteria are indicated by root mean square error (RMSE) and regression coefficient (R^2).

	SMR	SMX	SMM	TMP	CLA	AZI	ROX	LEV	FLU	NO_3- N	PO_4- P
H. pluvialis											
μ_{max} (day^{-1})	0.28 ± 0.02	0.15 ± 0.03	0.24 ± 0.04	0.21 ± 0.01	0.44 ± 0.06	0.05 ± 0.001	0.65 ± 0.012	0.21 ± 0.012	0.24 ± 0.02	0.26 ± 0.032	0.25 ± 0.034
k_s (μg L^{-1})	3.3	6.4	11.56	11.05	63.23	6.59	103.7	12.24	21.54	*2.79	*13.52
μ_{max}/ k_s ratio	0.084	0.024	0.011	0.021	0.019	0.042	0.017	0.007	0.006	0.093	0.019
RMSE (day^{-1})	0.32	0.31	0.3	0.3	0.3	0.37	0.3	0.3	0.3	0.3	0.3
R^2	0.92	0.95	0.5	0.54	0.69	1	0.41	0.55	0.58	0.33	0.47
Doubling time (days)	2.49	4.59	2.9	3.23	1.59	14.27	1.06	3.31	2.88	2.67	2.76
S. capricornutum											
μ_{max} (day^{-1})	0.11 ± 0.001	0.08 ± 0.001	0.08 ± 0.002	0.08 ± 0.007	0.07 ± 0.005	0.08 ± 0.006	0.08 ± 0.001	0.09 ± 0.002	0.07 ± 0.003	0.05 ± 0.002	0.08 0.001
k_s (μg L^{-1})	−1.66	−6.2	−7.87	−15.05	−15.63	−13.31	−15.47	−9.5	−15.49	*-9.79	*-8.86
μ_{max}/ k_s ratio	−0.065	−0.013	−0.005	−0.010	−0.005	−0.327	−0.009	−0.006	−0.005	−0.005	−0.009
RMSE (day^{-1})	0.3	0.31	0.29	0.93	0.28	0.28	0.28	0.3	0.41	0.29	1.31
R^2	1	0.89	0.87	0.92	0.81	0.8	0.73	0.71	0.88	0.64	0.94
Doubling time (days)	6.43	8.59	9.24	8.95	9.3	8.92	9.21	7.87	9.24	15.37	8.53
S. quadricauda											
μ_{max} (day^{-1})	0.28 ± 0.01	0.2 ± 0.03	0.22 ± 0.04	0.21 ± 0.07	0.22 ± 0.10	0.2 ± 0.08	0.21 ± 0.06	0.21 ± 0.05	0.26 ± 0.05	1.29 ± 0.12	0.2 ± 0.009
k_s (μg L^{-1})	17.19	8.53	13.7	23.38	26	19.46	22.32	20.63	41.17	*145.4	*12.26
μ_{max}/ k_s ratio	0.016	0.023	0.006	0.016	0.009	0.008	0.010	0.010	0.009	0.009	0.016
RMSE (day^{-1})	0.25	0.25	0.25	0.25	0.25	0.25	0.25	0.25	0.25	0.26	0.25
R^2	0.52	0.47	0.49	0.54	0.41	0.44	0.52	0.53	0.53	0.69	0.03
Doubling time (days)	2.48	3.53	3.12	3.29	3.16	3.39	3.33	3.32	2.63	0.54	3.47
C. vulgaris											
μ_{max} (day^{-1})	0.31 ± 0.02	0.31 ± 0.04	0.31 ± 0.03	0.31 ± 0.02	0.31 ± 0.04	0.31 0.01	0.31 ± 0.11	0.31 ± 0.03	0.31 ± 0.07	0.3 ± 0.08	0.3 ± 0.009
k_s (μg L^{-1})	0.22	0.22	0.29	0.17	0.36	0.3	0.16	0.07	0.29	*0.26	*0.25
μ_{max}/ k_s ratio	1.391	1.397	1.078	1.080	1.855	3.320	4.495	1.047	1.899	1.142	1.203
RMSE (day^{-1})	0.53	0.53	0.53	0.53	0.53	0.53	0.53	0.53	0.53	0.53	0.53
R^2	0.7	0.8	0.73	0.99	0.78	0.83	0.96	1	0.92	0.91	0.98
Doubling time (days)	2.22	2.22	2.22	2.25	2.22	2.23	2.25	2.26	2.24	2.35	2.33

* Units for NO_3- N and PO_4- P nutrients are mg L^{-1}.

the light of EAWAG-BBD prediction and previous reports. Based on the identified TPs, TMP transformation pathway is proposed (Fig. 4). TMP may transform into TP306-1 [*m/z* 307.1362] through hydroxylation (Pathway I). TP306-1 was the most prevalent biotransformation product of TMP, detected in all four algal batch cultures. TP306-1 was also reported as a primary metabolite of TMP in the bacterial and biological treatment processes (Jewell et al., 2016; Eichhorn et al., 2005). TP306-1 may transform into TP290-1 [*m/z* 291.1049] and TP290-2 [*m/z* 291.1049] via demethylation and oxidation processes. Jewel et al. also reported the transformation of TP306-1 into TP290-1 (Jewell et al.,

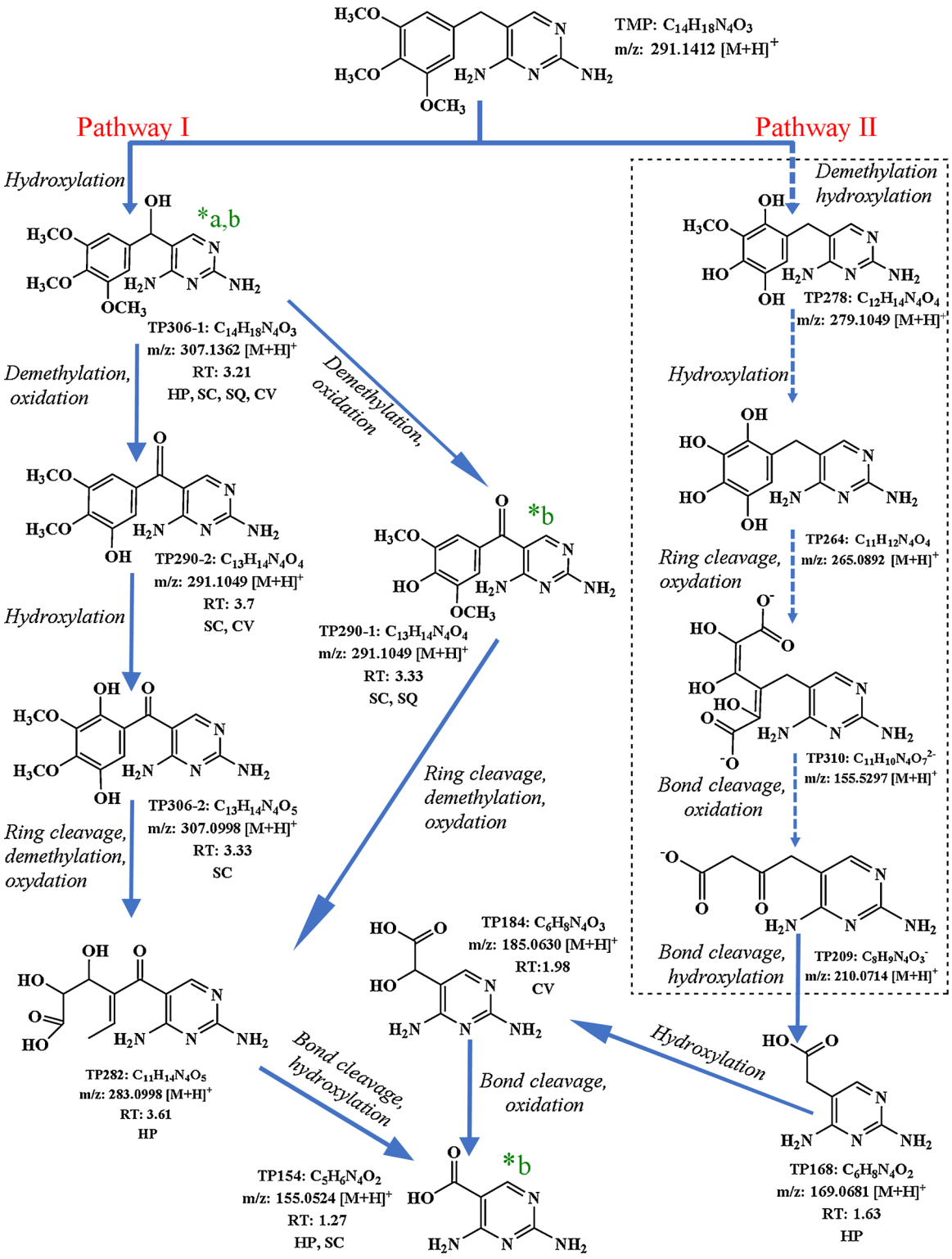

Fig. 4. The proposed metabolites and biotransformation pathway of TMP. Solid lines indicate the following proposed metabolites detected by QTOF, dotted lines and boxes indicate the intermediate transformation products predicted by EAWAG-BBD but not detected in this study. The direction of the arrows indicate the transformation path. *a (Eichhorn et al., 2005), *b (Jewell et al., 2016); RT (retention time); HP (*Haematococcus pluvialis*); SC (*Selenastrum capricornutum*); SQ (*Scenedesmus quadricauda*); CV (*Chlorella vulgaris*).

2016). TP290-1 can also directly transform into TP282 by ring cleavage, demethylation and oxidation. While, TP290-2 may undergo transformation into TP306-2 [*m/z* 307.0998] through hydroxylation that subsequently transforms into TP282 [*m/z* 283.0998] by ring cleavage, demethylation and oxidation. Subsequently, C—C bond cleavage and hydroxylation of TP282 may lead to the formation of TP154 [*m/z* 155.0524]. TMP can also undergo transformation into TP168 [*m/z* 169.0681] through a series of intermediates predicted by EAWAG-BBD as proposed in Pathway II. However, these intermediates were not detected in our study. Later, the hydroxylation of TP168 may form TP184 [*m/z* 185.0630] that can undergo C—C bond cleavage and hydroxylation to give TP154. TP154 was also reported as a direct hydrolytic product of TP290-1 in an earlier study (Jewell et al., 2016). Detection of a variety of TPs clearly indicate the complicated mechanisms and diverse pathways by microalgae for the breakdown of TMP.

Another two metabolites, TP126 and TP306-3 were also detected in the batch culture samples. TP126 [*m/z* 127.035] can be ascribed to sulfonamide antibiotics SMR, SMX, or SMM with the proposed pathways shown in Fig. S11. TP126 was also reported earlier as a degradation product of sulfamethazine and SMX by *Scenedesmus obliquus* (Xiong et al., 2019b). According to EAWAG-BBD, LEV can undergo transformations into *m/z* 379.1504 by ring cleavage and dehydroxylation and into *m/z* 321.1086 through bond cleavage and oxidation. Subsequently, *m/z* 321.1086 can yield TP306-3 [*m/z* 307.0929] by demethylation detected in this study. The proposed LEV transformation pathway is presented in Fig. S12.

In the present study, a variety of mechanisms viz. hydroxylation, amination, deamination, oxidation, demethylation, ring cleavage, etc. were involved in the transformation of antibiotics. As only small fractions of antibiotics were bioadsorbed, bioaccumulated, or abiotic degraded, therefore, the removal of majority of the antibiotics can be attributed to the biodegradation. Variations in the TPs suggest different mechanisms involved in the degradation of the antibiotics by different algal species. Detection of majority of metabolites in *H. pluvialis* batch culture can be attributed to enzymes as well as the production of astaxanthin that has strong scavenger antioxidant activity (Lee et al., 2019) to catalyze the degradation process. The rate of degradation may also be related to the efficacy of the enzymes against different structural vulnerabilities of the organic compounds.

3.7. Risk assessment of the TPs

The acute and chronic toxicity thresholds for the antibiotics and their respective TPs are presented in Table S8. The values for lethal concentration (LC_{50}), effective concentration (EC_{50}) and chronic value (ChV) for the major environmental food web organisms viz. fish, daphnid and green algae were determined by using ECOSAR (v2.0) (Reuschenbach et al., 2008; Sanderson et al., 2003). Generally, the TPs showed less toxicities compared to their parent compounds. However, exception was observed in the sulfonamides, where, TP126 showed higher acute toxicities for fish and green algae and higher chronic toxicity for green algae. Production of TPs with lower toxicities indicate the promise of microalgae as a potential bioremediation resource.

4. Conclusions

Microalgae demonstrated the removal of antibiotics and nutrients from synthetic wastewater in batch cultures, to qualify as a supplemental technology for the improvement of effluent quality. The antibiotic removal was mainly achieved by the biodegradation, while, bioadsorption, bioaccumulation and abiotic factors also contributed to minor extent. Monod kinetics was successful in explaining the role of contaminant removal in batch culture experiments with microalgae. *S. capricornutum* and *C. vulgaris* showed more affinity for the macrolides and fluoroquinolones than sulfonamides, while, *H. pluvialis* and *S. quadricauda* showed relatively higher preference for sulfonamides than the other antibiotic groups. Variations in the removal efficiencies as well as generation of different TPs by different algal species indicate variety of processes employed by algal species. Generally, the identified potential TPs showed overall less environmental risk than their respective parent compounds, indicating the potential of microalgae for use in the wastewater treatment systems. Further research is required to elucidate these processes with combinations of algal species at larger scales.

Authors' contributions

CK, AR and QS conceived and designed the study. CK, AR, YW, YL, and QZ performed experimental works. CK, AR and QS evaluated the data. CK, AR, CY, and QS wrote the manuscript. All authors read and approval to the final manuscript

Declaration of Competing Interest

The authors declare that there are no conflicts of interest.

Acknowledgments

We appreciated Ms. Shanshan Lin and Mr. Lifeng Lin for the instrument analysis guidance. This work was jointly funded by the Key projects for Inter-governmental Cooperation in Science, Technology and Innovation (2018YFE0103300), Distinguished Young Scholars of Fujian Province of Natural Science Foundation of Fujian Province (2017J06013), Science and Technology Planning Project of Xiamen (3502Z20182005), Water Environment Safety and Water Quality Assurance Center of Xiamen (WES&WQGE201903). Dr. Qian Sun appreciated the support from Youth Innovation Promotion Association CAS (2016280), Mr. Claude Kiki appreciated the scholarship from Chinese Scholarship Council (2017GXZ010423), and Dr. Azhar Rashid appreciated the fellowship from PIFI CAS (2017VEB0008).

Appendix A. Supplementary data

Supplementary material related to this article can be found, in the online version, at doi:https://doi.org/10.1016/j.jhazmat.2019.121985.

References

Aga, D.S., Lenczewski, M., Snow, D., Muurinen, J., Sallach, J.B., Wallace, J.S., 2016. Challenges in the measurement of antibiotics and in evaluating their impacts in agroecosystems: a critical review. J. Environ. Qual. 45, 407. https://doi.org/10.2134/jeq2015.07.0393.

Albero, B., Tadeo, J.L., Escario, M., Miguel, E., Pérez, R.A., 2018. Persistence and availability of veterinary antibiotics in soil and soil-manure systems. Sci. Total Environ. 643, 1562–1570. https://doi.org/10.1016/j.scitotenv.2018.06.314.

Angulo, E., Bula, L., Mercado, I., Montaño, A., Cubillán, N., 2018. Bioremediation of Cephalexin with non-living Chlorella sp., biomass after lipid extraction. Bioresour. Technol. 257, 17–22. https://doi.org/10.1016/j.biortech.2018.02.079.

Arpin-Pont, L., Bueno, M.J., Gomez, E., Fenet, H., 2016. Occurrence of PPCPs in the marine environment: a review. Environ. Sci. Pollut. Res. Int. 23, 4978–4991. https://doi.org/10.1007/s11356-014-3617-x.

Ashfaq, M., Li, Y., Wang, Y., Chen, W., Wang, H., Chen, X., Wu, W., Huang, Z., Yu, C.P., Sun, Q., 2017. Occurrence, fate, and mass balance of different classes of pharmaceuticals and personal care products in an anaerobic-anoxic-oxic wastewater treatment plant in Xiamen, China. Water Res. https://doi.org/10.1016/j.watres.2017.07.014.

Bai, X., Acharya, K., 2017. Algae-mediated removal of selected pharmaceutical and personal care products (PPCPs) from Lake Mead water. Sci. Total Environ. https://doi.org/10.1016/j.scitotenv.2016.12.192.

Burns, P.N., Becher, H., Burns, P.N., Becher, H., 2012. Methods for quantitative analysis. Handb. Contrast Echocardiogr. 153–171. https://doi.org/10.1007/978-3-642-59748-0_4.

Cheng, J., Li, K., Yang, Z., Zhou, J., Cen, K., 2016. Enhancing the growth rate and astaxanthin yield of Haematococcus pluvialis by nuclear irradiation and high concentration of carbon dioxide stress. Bioresour. Technol. 204, 49–54. https://doi.org/10.1016/j.biortech.2015.12.076.

Converti, A., Del Borghi, A., Arni, S., Molinari, F., 1999. Linearized kinetic models for the simulation of the mesophilic anaerobic digestion of pre-hydrolyzed woody wastes. Chem. Eng. Technol. 22, 429–437. https://doi.org/10.1002/(SICI)1521-

4125(199905)22:5<429::AID-CEAT429>3.0.CO;2-5.
Daneshvar, E., Zarrinmehr, M.J., Hashtjin, A.M., Farhadian, O., Bhatnagar, A., 2018. Versatile applications of freshwater and marine water microalgae in dairy wastewater treatment, lipid extraction and tetracycline biosorption. Bioresour. Technol. 268, 523–530. https://doi.org/10.1016/j.biortech.2018.08.032.
Davis, R.W., Siccardi, A.J., Huysman, N.D., Wyatt, N.B., Hewson, J.C., Lane, T.W., 2015. Growth of mono- and mixed cultures of Nannochloropsis salina and Phaeodactylum tricornutum on struvite as a nutrient source. Bioresour. Technol. 198, 577–585. https://doi.org/10.1016/j.biortech.2015.09.070.
de Morais, M.G., Costa, J.A.V., 2007. Isolation and selection of microalgae from coal fired thermoelectric power plant for biofixation of carbon dioxide. Energy Convers. Manage. 48, 2169–2173. https://doi.org/10.1016/j.enconman.2006.12.011.
Du, Y., Wang, J., Li, H., Mao, S., Wang, D., Xiang, Z., Guo, R., Chen, J., 2018. The dual function of the algal treatment: antibiotic elimination combined with CO_2 fixation. Chemosphere. https://doi.org/10.1016/j.chemosphere.2018.07.163.
Dutta, S., Basak, B., Bhunia, B., Chakraborty, S., Dey, A., 2014. Kinetics of rapamycin production by Streptomyces hygroscopicus MTCC 4003. 3 Biotech 4, 523–531. https://doi.org/10.1007/s13205-013-0189-2.
Eguchi, K., Nagase, H., Ozawa, M., Endoh, Y.S., Goto, K., Hirata, K., Miyamoto, K., Yoshimura, H., 2004. Evaluation of antimicrobial agents for veterinary use in the ecotoxicity test using microalgae. Chemosphere 57, 1733–1738. https://doi.org/10.1016/j.chemosphere.2004.07.017.
Eichhorn, P., Ferguson, P.L., Pérez, S., Aga, D.S., 2005. Application of ion trap-MS with H/D exchange and QqTOF-MS in the identification of microbial degradates of trimethoprim in nitrifying activated sludge. Anal. Chem. 77, 4176–4184. https://doi.org/10.1021/ac050141p.
Eppley, R.W., Rogers, J.N., Mccarthy, J.J., 1969. Half saturation constants for uptake of nitrate and ammonium. Limnol. Oceanogr.
Fareed, A., Zaffar, H., Rashid, A., Maroof Shah, M., Naqvi, T.A., 2017. Biodegradation of N-methylated carbamates by free and immobilized cells of newly isolated strain Enterobacter cloacae strain TA7. Bioremediat. J. 1–9. https://doi.org/10.1080/10889868.2017.1404964.
Foflonker, F., Ananyev, G., Qiu, H., Morrison, A., Palenik, B., Dismukes, G.C., Bhattacharya, D., 2016. The unexpected extremophile: tolerance to fluctuating salinity in the green alga Picochlorum. Algal Res. 16, 465–472. https://doi.org/10.1016/j.algal.2016.04.003.
Gojkovic, Z., Lindberg, R.H., Tysklind, M., Funk, C., 2019. Northern green algae have the capacity to remove active pharmaceutical ingredients. Ecotoxicol. Environ. Saf. 170, 644–656. https://doi.org/10.1016/j.ecoenv.2018.12.032.
González-Camejo, J., Viruela, A., Ruano, M.V., Barat, R., Seco, A., Ferrer, J., 2019. Dataset to assess the shadow effect of an outdoor microalgae culture. Data Br. 25, 4–7. https://doi.org/10.1016/j.dib.2019.104143.
Goswami, R.C.D., Kalita, M.C., 2011. Scenedesmus dimorphus and Scenedesmus quadricauda : two potent indigenous microalgae strains for biomass production and CO2 mitigation - a study on their growth behavior and lipid productivity under different concentration of urea as nitrogen source. J. Algal Biomass Utln. 2, 42–49. http://jalgalbiomass.com/paper8vol2no4.pdf.
Guo, W.Q., Zheng, H.S., Li, S., Du, J.S., Feng, X.C., Yin, R.L., Wu, Q.L., Ren, N.Q., Chang, J.S., 2016. Removal of cephalosporin antibiotics 7-ACA from wastewater during the cultivation of lipid-accumulating microalgae. Bioresour. Technol. https://doi.org/10.1016/j.biortech.2016.09.036.
Hammershøj, R., Birch, H., Redman, A.D., Mayer, P., 2019. Mixture effects on biodegradation kinetics of hydrocarbons in surface water: increasing concentrations inhibited degradation whereas multiple substrates did not. Environ. Sci. Technol. 53, 3087–3094. https://doi.org/10.1021/acs.est.9b00638.
Hernández-López, J., Vargas-Albores, F., 2003. A microplate technique to quantify nutrients (NO2-, NO3-, NH4+ and PO43-) in seawater. Aquac. Res. 34, 1201–1204. https://doi.org/10.1046/j.1365-2109.2003.00928.x.
Jacques, M., 1949. The growth of bacterial cultures. Annu. Rev. Microbiol. 3, 371–394.
Jaén-gil, A., Hom-diaz, A., Llorca, M., Vicent, T., Blánquez, P., Barceló, D., Rodríguez-mozaz, S., 2018. An automated on-line turbulent flow liquid-chromatography technology coupled to a high resolution mass spectrometer LTQ-Orbitrap for suspect screening of antibiotic transformation products during microalgae wastewater treatment. J. Chromatogr. A 1568, 57–68. https://doi.org/10.1016/j.chroma.2018.06.027.
Jewell, K.S., Castronovo, S., Wick, A., Falås, P., Joss, A., Ternes, T.A., 2016. New insights into the transformation of trimethoprim during biological wastewater treatment. Water Res. 88, 550–557. https://doi.org/10.1016/j.watres.2015.10.026.
Khona, D.K., Shirolikar, S.M., Gawde, K.K., Hom, E., Deodhar, M.A., D'Souza, J.S., 2016. Characterization of salt stress-induced palmelloids in the green alga, Chlamydomonas reinhardtii. Algal Res. 16, 434–448. https://doi.org/10.1016/j.algal.2016.03.035.
Kong, W., Huang, S., Shi, F., Zhou, J., Feng, Y., Xiao, Y., 2018. Study on Microcystis aeruginosa growth in incubator experiments by combination of Logistic and Monod functions. Algal Res. 35, 602–612. https://doi.org/10.1016/j.algal.2018.10.005.
Kovárová-Kovar, K., Egli, T., 1998. Growth kinetics of suspended microbial cells: from single-substrate-controlled growth to mixed-substrate kinetics. Microbiol. Mol. Biol. Rev. 62, 646–666. http://www.ncbi.nlm.nih.gov/pubmed/9729604%0Ahttp://www.pubmedcentral.nih.gov/articlerender.fcgi?artid=PMC98929.
Lee, K.Y., Lee, S.H., Lee, J.E., Lee, S.Y., 2019. Biosorption of radioactive cesium from contaminated water by microalgae Haematococcus pluvialis and Chlorella vulgaris. J. Environ. Manage. 233, 83–88. https://doi.org/10.1016/j.jenvman.2018.12.022.
Li, Y., Rashid, A., Wang, H., Hu, A., Lin, L., Yu, C.-P., Chen, M., Sun, Q., 2018. Contribution of biotic and abiotic factors in the natural attenuation of sulfamethoxazole: a path analysis approach. Sci. Total Environ. 633, 1217–1226. https://doi.org/10.1016/j.scitotenv.2018.03.232.
Lv, M., Lo, C., Hsu, C.C., Wang, Y., Chiang, Y.R., Sun, Q., Wu, Y., Li, Y., Chen, L., Yu, C.P., 2018. Identification of enantiomeric byproducts during microalgae-mediated transformation of metoprolol by MS/MS spectrum based networking. Front. Microbiol. 9, 1–11. https://doi.org/10.3389/fmicb.2018.02115.
Mulder, C., Hendriks, A.J., 2014. Half-saturation constants in functional responses. Glob. Ecol. Conserv. 2, 161–169. https://doi.org/10.1016/j.gecco.2014.09.006.
Nagarajan, D., Kusmayadi, A., Yen, H.-W., Dong, C.-D., Lee, D.-J., Chang, J.-S., 2019. Current advances in biological swine wastewater treatment using microalgae-based processes. Bioresour. Technol. 121718. https://doi.org/10.1016/j.biortech.2019.121718.
Okpokwasili, G.C., Nweke, C.O., 2005. Microbial growth and substrate utilization kinetics. African J. Biotechnol. 5, 305–317.
Pala, A., Bölükbaş, Ö., 2005. Evaluation of kinetic parameters for biological CNP removal from a municipal wastewater through batch tests. Process Biochem. 40, 629–635. https://doi.org/10.1016/j.procbio.2004.01.060.
Reuschenbach, P., Silvani, M., Dammann, M., Warnecke, D., Knacker, T., 2008. ECOSAR model performance with a large test set of industrial chemicals. Chemosphere. 71, 1986–1995. https://doi.org/10.1016/j.chemosphere.2007.12.006.
Sanderson, H., Johnson, D.J., Wilson, C.J., Brain, R.A., Solomon, K.R., 2003. Probabilistic hazard assessment of environmentally occurring pharmaceuticals toxicity to fish, daphnids and algae by ECOSAR screening. Toxicol. Lett. 144, 383–395. https://doi.org/10.1016/S0378-4274(03)00257-1.
Santos Escapa, C., Nuno De Coimbra, R., Bermejo Paniagua, S., Otero Cabero, M., 2017. World' s largest science, technology & medicine open access book publisher comparative assessment of pharmaceutical comparative assessment of pharmaceutical removal removal from wastewater by the microalgae from wastewater by, the microalgae chlorella. Biol. Wastewater Treat. Resour. Recover. 99–117. https://doi.org/10.5772/66772.
Shi, X., Yeap, T.S., Huang, S., Chen, J., Ng, H.Y., 2018. Bioresource Technology Pretreatment of saline antibiotic wastewater using marine microalga. Bioresour. Technol. 258, 240–246. https://doi.org/10.1016/j.biortech.2018.02.110.
Stanier, R.Y., Kunisawa, R., Mandel, M., Cohen-Bazire, G., 1971. Purification and properties of unicellular blue-green algae (order Chroococcales). Bacteriol. Rev. 35, 171–205.
Sun, Q., Li, M., Ma, C., Chen, X., Xie, X., Yu, C.P., 2016. Seasonal and spatial variations of PPCP occurrence, removal and mass loading in three wastewater treatment plants located in different urbanization areas in Xiamen, China. Environ. Pollut. 208, 371–381. https://doi.org/10.1016/j.envpol.2015.10.003.
Sun, M., Lin, H., Guo, W., Zhao, F., Li, J., 2017. Bioaccumulation and biodegradation of sulfamethazine in Chlorella pyrenoidosa. J. Ocean Univ. China. https://doi.org/10.1007/s11802-017-3367-8.
Thies, F., Backhaus, T., Bossmann, B., Crimme, H., 1996. Xenobiotic biotransformation in unicellular green algae. Plant Physiol. 112, 361–370.
Välitalo, P., Kruglova, A., Mikola, A., Vahala, R., 2017. Toxicological impacts of antibiotics on aquatic micro-organisms: A mini-review. Int. J. Hyg. Environ. Health 220, 558–569. https://doi.org/10.1016/j.ijheh.2017.02.003.
Van Epps, A., Blaney, L., 2016. Erratum to: Antibiotic Residues in Animal Waste: Occurrence and Degradation in Conventional Agricultural Waste Management Practices (Current Pollution Reports, (2016), 2, 3, (135-155), 10.1007/s40726-016-0037-1). Curr. Pollut. Reports 2, 156. https://doi.org/10.1007/s40726-016-0040-6.
Wang, Y., Ho, S.H., Cheng, C.L., Guo, W.Q., Nagarajan, D., Ren, N.Q., Lee, D.J., Chang, J.S., 2016. Perspectives on the feasibility of using microalgae for industrial wastewater treatment. Bioresour. Technol. 222, 485–497. https://doi.org/10.1016/j.biortech.2016.09.106.
Wang, Y., Li, Y., Hu, A., Rashid, A., Ashfaq, M., Wang, Y., Wang, H., Luo, H., Yu, C.P., Sun, Q., 2018. Monitoring, mass balance and fate of pharmaceuticals and personal care products in seven wastewater treatment plants in Xiamen City, China. J. Hazard. Mater. 354, 81–90. https://doi.org/10.1016/j.jhazmat.2018.04.064.
Wang, Y., Sun, Q., Li, Y., Wang, H., Wu, K., Yu, C.-P., 2019. Biotransformation of estrone, 17β-estradiol and 17α-ethynylestradiol by four species of microalgae. Ecotoxicol. Environ. Saf. 180, 723–732. https://doi.org/10.1016/j.ecoenv.2019.05.061.
Xin, L., Hong-ying, H., Ke, G., Ying-xue, S., 2010. Effects of different nitrogen and phosphorus concentrations on the growth, nutrient uptake, and lipid accumulation of a freshwater microalga Scenedesmus sp. Bioresour. Technol. 101, 5494–5500. https://doi.org/10.1016/j.biortech.2010.02.016.
Xiong, J.Q., Kurade, M.B., Abou-Shanab, R.A.I., Ji, M.K., Choi, J., Kim, J.O., Jeon, B.H., 2016. Biodegradation of carbamazepine using freshwater microalgae Chlamydomonas mexicana and Scenedesmus obliquus and the determination of its metabolic fate. Bioresour. Technol. https://doi.org/10.1016/j.biortech.2016.01.038.
Xiong, J., Kurade, M.B., Jeon, B., 2017a. Biodegradation of levofloxacin by an acclimated freshwater microalga, Chlorella vulgaris. Chem. Eng. J. 313, 1251–1257. https://doi.org/10.1016/j.cej.2016.11.017.
Xiong, J.Q., Kurade, M.B., Patil, D.V., Jang, M., Paeng, K.J., Jeon, B.H., 2017b. Biodegradation and metabolic fate of levofloxacin via a freshwater green alga, Scenedesmus obliquus in synthetic saline wastewater. Algal Res. 25, 54–61. https://doi.org/10.1016/j.algal.2017.04.012.
Xiong, J.Q., Kurade, M.B., Jeon, B.H., 2018. Can Microalgae Remove Pharmaceutical Contaminants from Water? Trends Biotechnol. 36, 30–44. https://doi.org/10.1016/j.tibtech.2017.09.003.
Xiong, J., Govindwar, S., Kurade, M.B., Paeng, K., Roh, H., Ali, M., Jeon, B., 2019a. Chemosphere Toxicity of sulfamethazine and sulfamethoxazole and their removal by a green microalga, Scenedesmus obliquus. Chemosphere 218, 551–558. https://doi.org/10.1016/j.chemosphere.2018.11.146.
Xiong, J.Q., Kim, S.J., Kurade, M.B., Govindwar, S., Abou-Shanab, R.A.I., Kim, J.R., Roh, H.S., Khan, M.A., Jeon, B.H., 2019b. Combined effects of sulfamethazine and sulfamethoxazole on a freshwater microalga, Scenedesmus obliquus: toxicity, biodegradation, and metabolic fate. J. Hazard. Mater. 370, 138–146. https://doi.org/10.

1016/j.jhazmat.2018.07.049.
Xu, M., Bernards, M., Hu, Z., 2014. Algae-facilitated chemical phosphorus removal during high-density Chlorella emersonii cultivation in a membrane bioreactor. Bioresour. Technol. 153, 383–387. https://doi.org/10.1016/j.biortech.2013.12.026.
Zhou, G.J., Ying, G.G., Liu, S., Zhou, L.J., Chen, Z.F., Peng, F.Q., 2014. Simultaneous removal of inorganic and organic compounds in wastewater by freshwater green microalgae. Environ. Sci. Process. Impacts 16, 2018–2027. https://doi.org/10.1039/c4em00094c.